Journal of Biomedical Optics

SPIEDigitalLibrary.org/jbo

Functional adaptation of long bone extremities involves the localized "tuning" of the cortical bone composition; evidence from Raman spectroscopy

Kevin Buckley
Jemma G. Kerns
Helen L. Birch
Panagiotis D. Gikas
Anthony W. Parker
Pavel Matousek
Allen E. Goodship

SPIE

Functional adaptation of long bone extremities involves the localized "tuning" of the cortical bone composition; evidence from Raman spectroscopy

Kevin Buckley,[a,b,*] Jemma G. Kerns,[b] Helen L. Birch,[b] Panagiotis D. Gikas,[c] Anthony W. Parker,[a] Pavel Matousek,[a] and Allen E. Goodship[b]
[a]Central Laser Facility, Research Complex at Harwell, STFC Rutherford Appleton Laboratory, Harwell Oxford, OX11 0FA, United Kingdom
[b]University College London, Institute of Orthopaedics and Musculoskeletal Science, Stanmore, HA7 4LP, United Kingdom
[c]Royal National Orthopaedic Hospital, Stanmore, HA7 4LP, United Kingdom

Abstract. In long bones, the functional adaptation of shape and structure occurs along the whole length of the organ. This study explores the hypothesis that adaptation of bone composition is also site-specific and that the mineral-to-collagen ratio of bone (and, thus, its mechanical properties) varies along the organ's length. Raman spectroscopy was used to map the chemical composition of long bones along their entire length in fine spatial resolution (1 mm), and then biochemical analysis was used to measure the mineral, collagen, water, and sulfated glycosaminoglycan content where site-specific differences were seen. The results show that the mineral-to-collagen ratio of the bone material in human tibiae varies by <5% along the mid-shaft but decreases by >10% toward the flared extremities of the bone. Comparisons with long bones from other large animals (horses, sheep, and deer) gave similar results with bone material composition changing across tens of centimeters. The composition of the bone apatite also varied with the phosphate-to-carbonate ratio decreasing toward the ends of the tibia. The data highlight the complexity of adaptive changes and raise interesting questions about the biochemical control mechanisms involved. In addition to their biological interest, the data provide timely information to researchers developing Raman spectroscopy as a noninvasive tool for measuring bone composition *in vivo* (particularly with regard to sampling and measurement protocol). [DOI: 10.1117/1.JBO.19.11.111602]

Keywords: vibrational spectroscopy; Raman spectroscopy; bone; biology.

Paper 130846SSR received Nov. 28, 2013; revised manuscript received Jan. 10, 2014; accepted for publication Jan. 13, 2014; published online May 19, 2014.

1 Introduction

Bone is not a single material but a class of composites with varying proportions of mineral, organic material, and water, and consequently, a wide range of mechanical properties.[1] The composition of the material in a specific bone is determined by the functional demands placed on it; bone can have up to 90% mineral by weight if it is being naturally selected for maximal stiffness or as little as 50% if it is being selected for toughness.[1–3] Limb bones, in general, need to be both stiff and tough (fracture resistant) and, thus, have intermediate composition. Studies across a large number of species have shown limb bones to comprise ~65% mineral and ~35% organic material/water and to have similar material properties. For example, a variety of human, bovine, leopard, brown bear, roe deer, king penguin, polar bear, and wallaby limb bones have the Young's modulus in the range of 16.7 to 22.9 GPa.[1,4–7]

Other studies, however, have shown that even within a single bone, the mechanical properties of the cortical bone material can have measurable site-specific variations and that these differences can be dependent upon anatomical position. Mechanical and ultrasonic studies of elastic moduli and fracture stresses have been reported for many bone samples, including human, canine, and bovine femora, equine metacarpal bones, and bovine tibiae. These studies have shown that some mechanical properties of cortical bone have local extrema in the mid-shaft. For example, elastic moduli have a local maximum at the mid-shaft and decrease in both the proximal and distal directions along the cephalocaudal axes.[8–13] In addition to mechanical testing, some of these studies used Archimedes principle and/or gravimetric techniques to measure changes in the density, and/or mineral content, of the bone material at different points along the length of the bones in question. They found lower densities and lower mineral content toward the ends of the diaphyses (spatial resolution >10 cm).[11,12]

Some studies have focused solely on density variations at specific anatomical positions along the bone (four or five positions per bone); Archimedes principle has been employed to show that the density of the human femoral cortex varied from mid-shaft to metaphysis,[14] x-ray techniques have been used to study mineral density distributions along the femoral diaphysis of various primates,[15] and ultrasound measurements have shown regional stiffness differences along the entire length of human tibiae.[16] Investigators have also used x-ray tomographic techniques (spatial resolution ~30 mm) and chemical/gravimetric analysis to show gradients of decreasing bone density toward the distal end of rat femoral diaphyses.[17,18] However, it is not clear from these studies whether the variations in density and stiffness are due to architectural/microstructural differences, due to differing composition of the bone material, or due to both.

In parallel to measuring the relative ratio of mineral to collagen, Raman spectroscopy provides a means to measure the

*Address all correspondence to: Kevin Buckley, E-mail: kevin.buckley@stfc.ac.uk

changes in the degree of carbonate-for-phosphate substitution in the bone-apatite crystals (this is a feature of Raman that sets it apart from techniques used in the studies discussed above, i.e., x-ray, ultrasound, gravimetric, etc.). The phosphate-to-carbonate ratio has been shown to decrease with bone age and mineral crystallinity.[19] It has also been shown to correlate with some mechanical properties of bone material, e.g., studies of osteoporosis in humans[20] and aging in mice[21] have shown that both increased mineral-to-collagen ratio and decreased phosphate-to-carbonate ratio were significantly correlated with low trauma fracture (human osteoporosis) and decreased deformation capacity (aging in mice).

The aim of this study is to explore the hypothesis that the regional differences in structural architecture along a long bone are associated with changes in the chemical composition of the bone. In order to test the hypothesis, (nondestructive) Raman spectroscopy was used to map the mineral-to-collagen and phosphate-to-carbonate ratios of bone along excised human tibiae (and other bones) with fine spatial resolution (1 mm intervals). Biochemical analysis (of 250-mg sections) was then performed to measure the absolute composition of the bone where the site-specific differences were seen. The human tibia was the central focus of the study because its structure and anatomy has been well characterized in the past, and its anatomical structure has been shown to have regional variation that is closely adapted to the mechanical requirements (a relationship that remains regardless of the gender and anthropometric characteristics of the individual).[22] Long bones from other species (horses, sheep, and deer) were also used to confirm the general biological principle hypothesized.

2 Materials and Methods

2.1 *Bone Samples*

Five human tibiae from three individuals (one male and two females) of ages 58, 72, and 88 were obtained from the Vesalius Clinical Training Centre at the University of Bristol, with appropriate ethical approval and material transfer agreements. The tibiae were examined by an orthopedic surgeon and showed no signs of bone disease (deaths were due to soft-tissue cancers and stroke).

Additional long bones were collected from other species (metacarpal bones from Thoroughbred racehorses, the metacarpus of a 1-year-old red deer stag, and the femur of a skeletally mature Welsh Mule domestic sheep) were also studied in order to strengthen the biological significance of our hypothesis. All the bones were frozen after being excised and stored in a freezer (193 K). Soft tissue and periostea were removed with scalpels before spectroscopic examination.

2.2 *Raman Data Collection*

The Raman spectrometer used to collect the data was custom built by Cobalt Light Systems Ltd. (Oxfordshire, United Kingdom). It utilized an 830-nm near-infrared laser, which delivered 300 mW to the sample (1 mm spot size). The collection optics imaged the scattered light into the fiber-optic bundle and then into a spectrograph with a CCD detector (Andor iDus 420 BR-DD, Belfast, Northern Ireland) at its output. To aid overall collection efficiency, the low-loss Optran WF fiber bundle used a round configuration of 33 fibers to collect the filtered Raman signal; the spectrograph end of the fiber bundle was configured as a linear array to optimally fill both the spectrograph input slit and the available vertical extent of the CCD. The detector had a spectral resolution of $\sim 8\ \mathrm{cm}^{-1}$, and its software removed spurious signals that were due to cosmic-ray events.

The spectrum-collection process was automated by loading the bones on a motorized translation stage that was controlled by the instrument's software. The software enabled automated movement of the sample stage and acquisition of Raman spectra. The flat medial surface of each tibia was then scanned along the full length of the shaft; a 30-s spectrum (30×1 s accumulations) was taken at each step (every 1 mm). The cranial surfaces of the horse, sheep, and deer bones were scanned in the same way. The order of the measurements was randomized to negate the influence of instrumental and environmental drifts. The optical setup of the instrument and the scattering/absorption properties of near-infrared light meant all the Raman signal that was collected originated from within ~1 to 2 mm of the scanned surface.

In some of the previous mechanical and ultrasonic studies discussed above, the variation of elastic moduli and fracture stresses along the cephalocaudal axis were ascribed to the anisotropic manner in which the osteons are orientated in the bone material.[10,11] Unlike some studies previously reported in the literature,[23,24] the Raman spectrograph in the present study was largely insensitive to orientation/polarization effects (it had no polarizer, a large spot size, utilized optical fibers, and had low numerical aperture[25]). The instrument's insensitivity to polarization was confirmed by probing highly aligned tendon samples at different orientations and also by comparing different Raman band ratios from bone samples (i.e., the variation in the phosphate ν_1/amideI ratio and the variation in phosphate ν_4/amideIII ratio).[23]

2.3 *Raman Data Processing*

The variable sensitivity of the Cobalt instrument (i.e., of the filters and detector) across the spectral range was corrected using an HgAr calibration lamp. The broad fluorescence backgrounds of the bone spectra were removed using a polynomial fitting routine (script written in-house on MATLAB®, The Mathworks Inc., version 2007b).[26]

The mineral-to-collagen ratios were determined by comparing band heights [phosphate $\nu 1$ band ($\sim 960\ \mathrm{cm}^{-1}$) for mineral and proline/hydroxyproline bands (average height across the band envelope ~830 to 900 cm^{-1}) for collagen] and were normalized to 100% (divided by the mean) for the compositional trend plots. The phosphate-to-carbonate ratio was calculated by dividing the phosphate $\nu 1$ band intensity by the carbonate band ($\sim 1070\ \mathrm{cm}^{-1}$) intensity (illustrated in Fig. 2 of Ref. 21).

The trend plots (Figs. 3, 4, and 6) were smoothed with the use of rolling averages (each data point is the average of a spectrum and two neighbors on either side) and averaged using an interpolation function (OriginLab, OriginPro 8.5).

2.4 *Analysis of Bulk Composition*

The data in Fig. 2(b) was collected with a Renishaw *inVia* Raman microscope (×5 Leica objective) with an 830-nm laser that produced 100 mW at sample (Renishaw, Gloucestershire, United Kingdom). One of the human tibiae (from a 58-year-old male) was sectioned after the other data had been collected, and it was divided in half along the coronal plane so as to expose the full thickness of the cortex for further

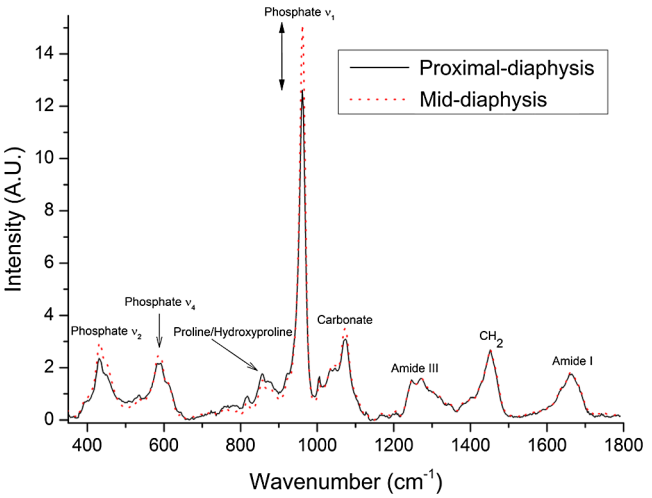

Fig. 1 Raman spectra of human tibial bone. The bone halfway along the tibia (red dotted spectrum) has a greater mineral-to-collagen ratio than that from a more proximal part of the cortex [the black spectrum is taken 80% along the length of the bone (from distal end)].

spectroscopic examination. Ten spectra were collected from the cortex at four anatomical positions (distal end, proximal end, and two near the mid-shaft); the spectra were collected in a line across the full cortex (from the periosteal surface to the endosteal surface). The data were processed in the same way as above.

2.5 *Biochemical Analysis*

2.5.1 *Water content*

Following the collection of Raman spectra, sections of cortical bone (0.15 cm^3, ~250 mg) were cut from four equally spaced points along the anterio-medial aspect of the human tibia, i.e., the two ends of the diaphysis and two points in the middle, dividing the diaphysis into thirds. The medullary surface of the bone samples was scraped clean of any cancellous bone and weighed accurately on a digital balance, frozen at −80°C, and dried to a constant weight under vacuum in a freeze dryer (Edwards, Crawley, England). The samples were reweighed accurately on a digital balance and the water content calculated as percentage of the wet weight.

2.5.2 *Mineral content*

Following lyophilization, the samples were defatted by suspending in 5 ml acetone at room temperature with shaking for 1 h. The defatting step was repeated three times. Samples were then washed twice with 5 ml of deionized (DI) water for 30 min at room temperature, frozen at −80°C, and redried in the freeze drier. The defatted, lyophilized samples were ground to a powder in a mikro-dismembrator (Sartorius, Germany) set at 3000 rpm for 1 min prior to demineralization. Samples were weighed accurately and 10% ethylenediamine tetra-acetic acid (EDTA), pH 7.5 added (4 mg bone/ml). Demineralization was carried out for 6 days at 4°C with agitation. After this time, the samples were centrifuged at 4600g and the supernatant removed. Samples were washed with 5 ml of DI water, centrifuged, and the supernatant removed prior to lyophilization in the freeze drier. The dry weight was then accurately recorded and an approximate mineral content calculated. Mineral content is expressed as percentage of the wet weight of bone.

2.5.3 *Collagen and sulfated glycosaminoglycan content*

Demineralized bone sample was solubilized by papain digestion as described previously.[27] To determine collagen content, a 100-μl aliquot of the papain digest was hydrolyzed in 6 M HCL at 110°C for 24 h. The hydrolysate was evaporated to dryness in a SpeedVac Concentrator (SPD131DDA, Thermo Fisher Scientific, Loughborough, England) and redissolved in DI water. Collagen content was determined by measuring the amino acid hydroxyproline as described previously.[27] Hydroxyproline concentrations were calculated by comparison

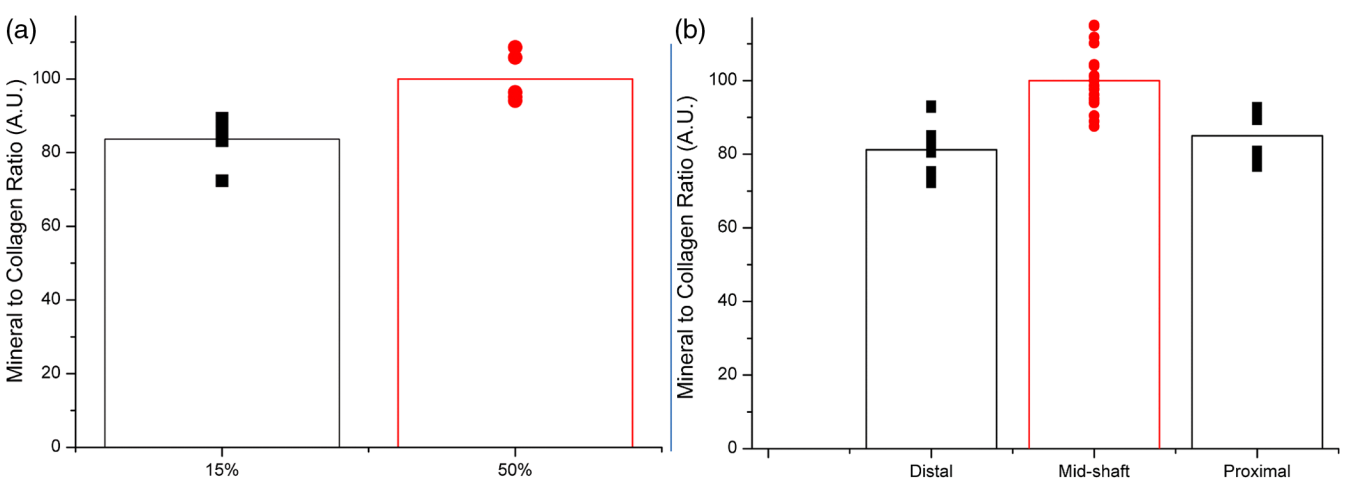

Fig. 2 (a) The histogram shows the average of the five tibiae. The ratio of mineral to collagen is smaller near the end of the tibia (15% from distal end) than at mid-shaft (50% from distal end). (b) The bulk bone composition across the full thickness of the tibial cortex. Ten spectra were collected from the cortex at four anatomical positions (distal end, proximal end, and two near the mid-shaft); the spectra were collected in a line from the periosteal surface to the endosteal surface of a sectioned human tibia.

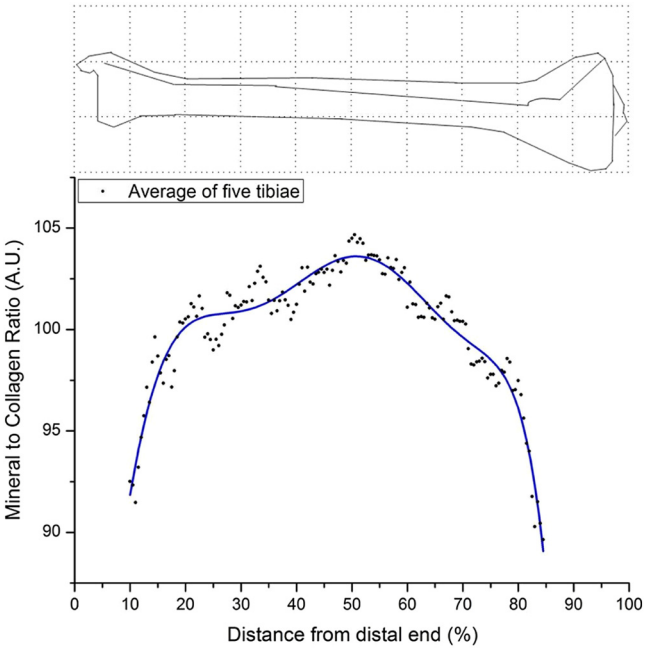

Fig. 3 Mineral-to-collagen ratio along the length of the human tibia; the bone near the mid-shaft has a larger mineral-to-collagen ratio than bone nearer the metaphysis (mean of five tibiae).

with a standard curve prepared with standards (0 to 10 μg hydroxyproline/ml) and collagen content calculated assuming hydroxyproline to be present at 14%. Collagen content is expressed as a percentage of the wet weight of bone tissue.

Total sulfated glycosaminoglycan (GAG) content was quantified in aliquots of the papain digest by the method of Farndale et al. using dimethylmethylene blue dye.[28] Concentrations were calculated by comparison with a standard curve prepared with purified bovine trachea chondroitin sulfate (0 to 100 μg/ml). Results are expressed as μg chondroitin sulfate equivalent sulfated GAG/mg dry demineralized bone tissue.

3 Results

3.1 *Raman Spectroscopy*

Typical Raman spectra of human tibial bone are shown in Fig. 1; the spectra are very similar, but inspection of the mineral bands (phosphate and carbonate bands) shows that the bone from the mid-shaft (halfway along the bone) has a higher ratio of mineral-to-collagen than bone from a more proximal region (spectrum was taken from point 80% along the total length of the tibia, measured from distal end). Figure 2(a) shows that a similar difference can be seen at the distal end of the tibia; this time the values are shown for five human tibiae. The average mineral-to-collagen ratio for the mid-shaft tibial bone is ~20% higher ($p < 0.005$) than that found ~7 cm from the knee (15% of the total length from the distal end). Figure 2(b) shows that this difference is not a surface effect and that the ~20% difference in mineral-to-collagen ratio holds across the thickness of the cortex ($p < 0.005$).

When the mineral-to-collagen ratio is measured at hundreds of points along the cephalocaudal axis, a macroscopic-scale structure is revealed; the mineral-to-collagen ratio along the mid-section of the diaphysis is relatively stable (from ~25 to ~75% of the total tibia length the ratio varies by ~5%),[29] but in the extremities, the mineral-to-collagen ratios decrease by 10% and keep decreasing (Fig. 3). Figure 4 shows similar macroscopic scale mineralization patterns in the distal cortices of equine metacarpal bones, the distal cortex of an ovine femur, and along the whole length of a cervine metacarpal bone.

The mineral-to-collagen ratio of the tibia (measured with Raman spectroscopy) was compared with structural and architectural properties previously published by Capozza et al.[22] The Capozza data were normalized to 100 (%) and plotted against similarly treated Raman data (Fig. 5). The comparison revealed a simple relationship between the mineral-to-collagen ratio and the thickness of the cortex, with the thinner areas being the ones with lowest ratio of mineral-to-collagen [Fig. 5(a)]. The analysis also showed more complicated relationships [Fig. 5(b)] between the mineral-to-collagen ratio and the bone mineral content, the circularity of the bone, and the cross-sectional moment of inertia. Below mineral-to-collagen ratio of 100 (i.e., below average), the structural properties adopt either one of two distinct values; these data points all come from the ends of the bones. Above mineral-to-collagen ratio of 100 (i.e., above average), the structural properties adopt wider range of values (these data points come from the mid-shaft).

The variation in the phosphate-to-carbonate ratio along the length of the tibia is shown in Fig. 6. The pattern has similarities with the mineral-to-collagen ratio profile in Fig. 3 in that it is reasonably uniform along the mid-shaft (<3%) but decreases (by 6%) toward the ends of the bone. There are, however, differences between the phosphate-to-carbonate pattern and

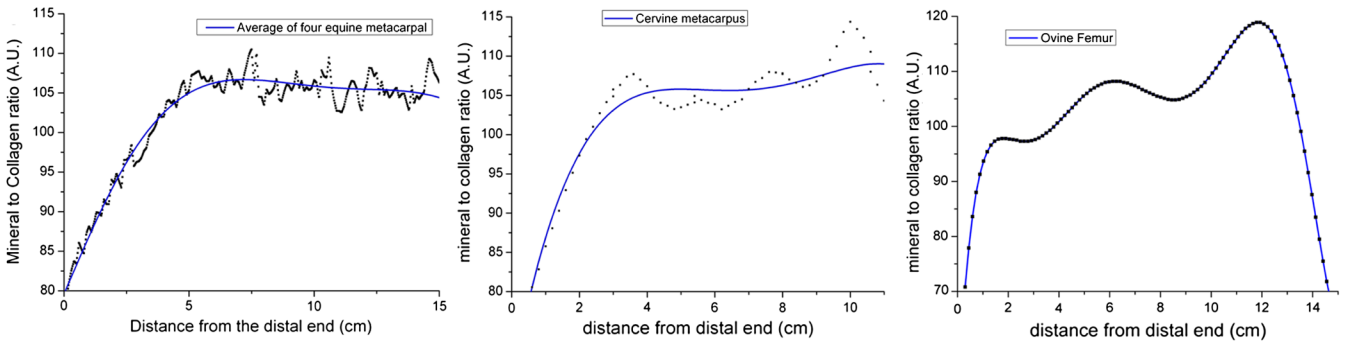

Fig. 4 Mineral-to-collagen ratio along the length of various long bones. (a) The distal end (65% of the length, proximal end not shown) of four equine metacarpal-bone cortices (mean). (b) The distal end (75% of the length, proximal end not shown) of a cervine metacarpal-bone cortex. (c) The whole cortex of an ovine femur.

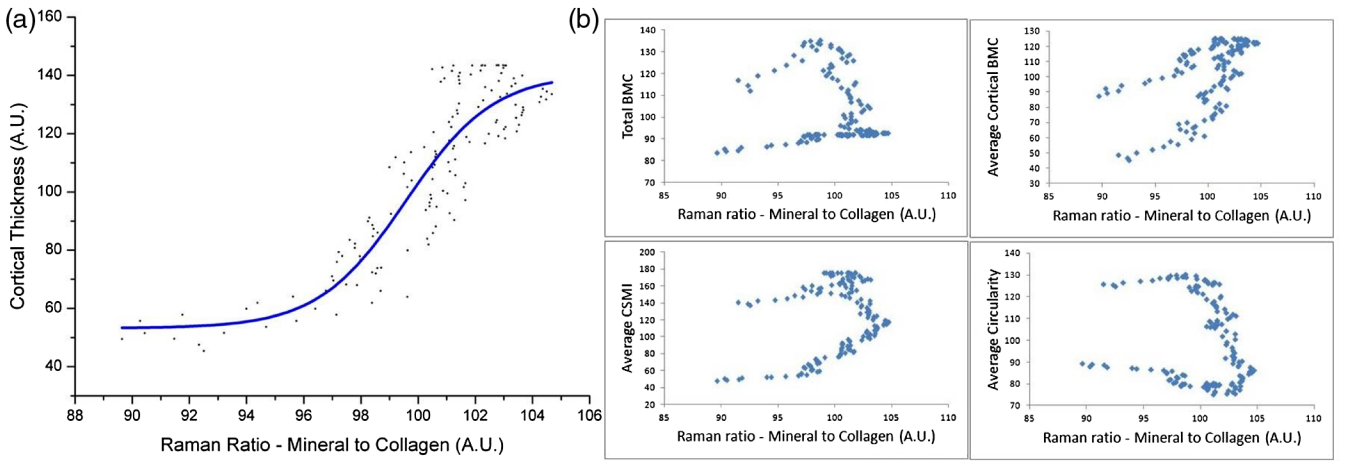

Fig. 5 Mineral-to-collagen ratio versus structural/architectural properties[22] of the human tibia; (a) as the cortex of the human tibia increases, the mineral-to-collagen ratio of bone material also increases. (b) The bone mineral content (BMC), cross-sectional moment of inertia (CSMI), and circularity have similar (more complicated) relationships with the Raman ratio. They each have two extreme values when the mineral-to-collagen is less than 100 (corresponding to the two ends of the tibia), and a range of values when the mineral-to-collagen is greater than 100 (corresponding to mid-shaft). All structural data from Capozza et al.[22]

the mineral-to-collagen pattern; by comparing Fig. 6 with Fig. 3, it can be seen that the carbonate substitution does not vary as much as the mineralization (note figures are plotted on the same scale); also the decrease of the phosphate-to-carbonate ratio at the proximal end of the bone begins nearer the midpoint of the bone and decreases more slowly.

3.2 *Biochemical Analysis*

The results of the biochemical analyses are shown in Fig. 7(a). The mineral content of the bone samples, calculated by the weight change following extraction with EDTA, was 68.4% ± 6.0 (mean ± SD) and levels showed regional variation that agreed with the Raman data. The water content ranged from 2.6 to 18.8% (7.5% ± 4.1) and was lower in the mid-diaphysis than at the diaphysis ends. Collagen content showed a reverse pattern of that seen in the mineral content along the diaphysis (17.4% ± 3.9). Those regions of bone with the highest mineral content had the lowest sulfated GAG content in the organic component.

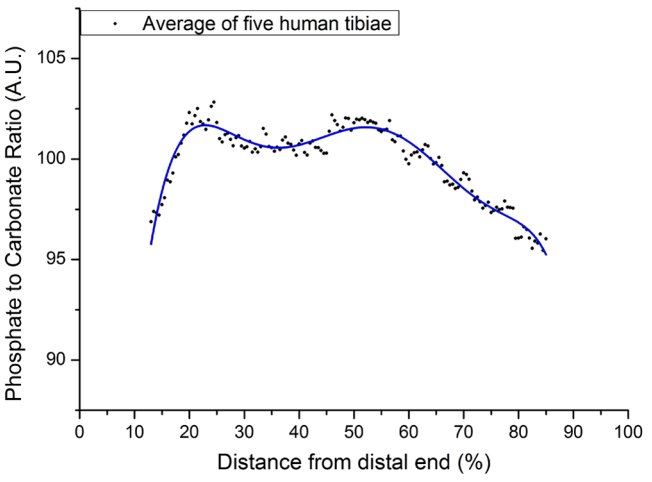

Fig. 6 The composition of the bone apatite is not uniform along the length of the human tibia (average of five tibiae); the ratio of phosphate to carbonate is larger near the mid-shaft than toward the metaphyses.

Figure 7(b) shows a version of the ternary diagrams similar to those in Refs. 1 and 6; the shaded gray area roughly corresponds to the area where all the bones found in nature would lie. In this ternary diagram, the bone is from different regions of the human tibia rather than functionally adapted bones from different species (that are plotted in the Refs. 1 and 6). The tibia samples spread across the shaded area with the mid-shaft samples clustering toward the highly mineralized corner and the proximal/distal samples clustering toward the antler end where less mineralized bones are found.[1,6]

4 Discussion

The bone material that comprises the cortices of long bones is not uniform; it has varying ratios of mineral-to-collagen and phosphate-to-carbonate (bone apatite composition), which change as a function of position along the cephalocaudal axis. Both the mineral-to-collagen ratio and the phosphate-to-carbonate ratio vary by <5% along the mid-shaft but decrease toward the flared extremities of the bone. The changing proportions of mineral and collagen are consistent with gravimetric, mechanical property and density variations, which have been measured in the past,[8,10–12,14–18] but the Raman spectroscopy technique has revealed, for the first time, how complex the adaption is, with bone composition varying over a distance of millimeters.

4.1 *Raman Spectroscopy of Whole Bones*

Raman spectroscopic techniques have been used to create spatial maps of chemical changes in bones in a number of different studies; these include studies of undamaged, strained, and failed regions of bone, developing murine skulls, and across individual osteons.[30–32] Raman spectroscopy has also been used to investigate composition variation within the cortices of individual bones; a study looking at the mechanical property variation between cranial and caudal quadrants of a murine femur found that the composition did not differ between the two

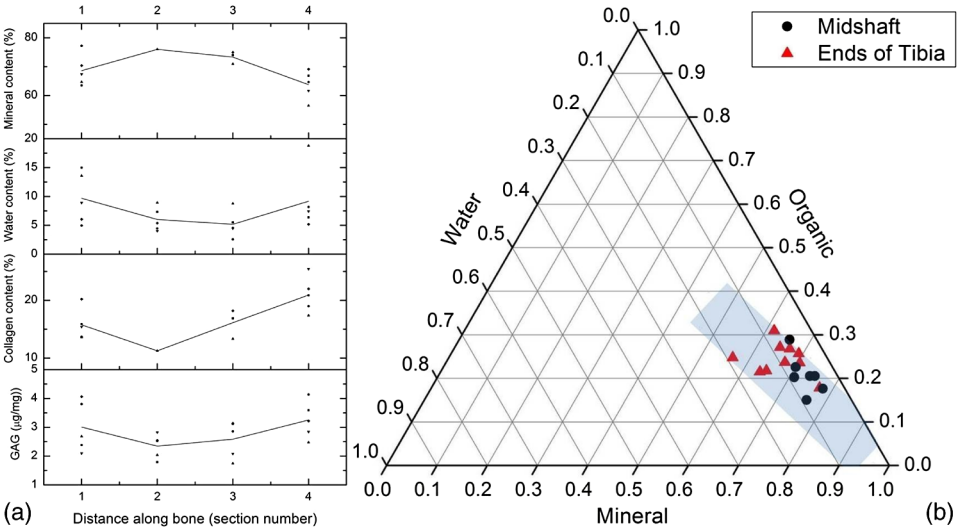

Fig. 7 (a) The biochemistry results show the percentage of mineral, water, and collagen for different samples of bone taken at different points along the length. The fraction of glycosaminoglycan (μg per mg of dry demineralized bone) is also shown. (b) These results are summarized in this ternary diagram, which shows the relative proportions, by weight, of the main constituents of human tibia bone; mid-shaft specimens are represented as circles and specimens from the proximal and distal ends of the bone are represented as triangles. All the bones in nature would lie near the shaded area.

but that the orientation of the collagen fibrils did.[33] Other studies looked at the mechanical property and Raman spectral differences between newly formed bone near, and older bone further from, the periosteum[34] and at the differences between cubes of metaphyseal bone and diaphyseal bone.[35] Typically, these experiments mapped much smaller areas and length scales than those we report here.

In Sec. 3, it was stated that the composition of the bone along the mid-section of the diaphysis is relatively stable (from ~25 to ~75% of the total tibia length the ratio varies by ~5%); our group has recently published a paper that quantified this mid-shaft compositional variation; we showed that across 10 cm of diaphyseal (mid-shaft) cortical bone, the phosphate-to-amide I ratio can vary by as much as 8%, and the phosphate-to-carbonate ratio by as much as 5%.[29] Both this study and the Raman tomographic imaging of large, intact sections of a canine limb bone, which have been reported by another group,[36] differ from the present study in that they did not look for variations at the macroscopic scale along (the cephalo-caudal axis of) the entire bone.

4.2 *Regional Variation of Mineralization in Long Bones*

Long bones grow in length from the growth plates (physeal plates) at each end; bone material that is furthest from a growth plate has (if we neglect remodeling for the present) taken longer to mature and should have reached a later stage of mineralization. These differences in the age of the bone material have been used to explain findings from an x-ray tomographic study of mineralization gradients in the femora of 6- to 9-week-old rats[18] and a Raman study that showed differences between metaphyseal bone and diaphyseal bone from the femora of 2- to 12-week-old mice.[35] Distance from the growth plate is not as relevant to most of the data presented here as all the bones were obtained from skeletally mature individuals [the exception being the red deer stag in Fig. 4(b), which did show the same pattern but was only 1 year old].

If more remodeling were to occur near the ends of long bones, the bone material there would, on average, be younger than the mid-diaphysis bone (and the associated resorption cavities would also contribute to lowering the density). There have been studies that show that this is the case in dogs.[37–39] In Marotti's study, skeletons of stray dogs were collected and various long bones (metacarpal bone, metatarsal bone, femur, ulna, rib, etc.) were sectioned and examined histologically. He found that there were more secondary osteons per unit area near the ends of the bones than nearer the mid-shaft.[38] In younger animals, this phenomenon has been ascribed to the conversion of the endosteal surface of the cortex to trabecular bone in growing bones.[40] The Raman and biochemical data in the current study were taken across the cortex (rather than just the endosteal surface), but the site-specific remodeling described by Marotti may still be relevant.

It has long been proposed that the density patterns along long bones are a structural feature of developmental origin, with the density increasing as an adaptation to mechanical loading.[14,15] These density patterns could also be due to site-specific remodeling or they could be related to the site-specific adaptation of the mineral content of bone.

4.3 *Compositional Variation and Material Properties*

Much of the variation in mechanical properties along the length of bones (particularly the variation in tensile strength) is due to variation in collagen fibril orientation.[10,11,33,41] However, the difference in the mineral-to-collagen ratio could also have a functional significance, for instance, a decrease in the mineral-to-collagen ratio of 10% could be expected to lead to a 7.5 to 10% decrease in the Young's modulus.[3] This may be beneficial to the function of the tibia if in regions where loads were transferred from one bone to the next, the cartilage was protected from destructive forces. Cortical bone material and the

cancellous bone material are more pliant (less stiff) and more able to absorb energy (tough) when they have lower mineral-to-collagen ratios. Excepting the complications introduced by microstructure[42] and remodeling, this has already been shown for cancellous bone material (the trabeculae do have a lower mineral volume fraction,[42,43] a smaller mineral-to-collagen ratio as measured with Raman spectroscopy,[44] and the material is 20 to 30% less stiff than cortical bone[43,45]).

Les et al.,[8] investigating the distribution of material properties in equine metacarpal bones, suggested that the variations were adaptive, concluding that they served to enhance and modulate sagittal bending; however, they were unable to address whether the cephalocaudal variation was the result of adaptation to applied loads or was genetically determined, independent of exercise regimes.[8]

4.4 *Raman Spectroscopy and Biochemical Analysis*

It was shown some time ago that the mineral content of bone (as measured with ashing) is correlated with the phosphate-to-amide I ratio (as measured with FTIR).[46] It has also been shown that Raman mineral-to-collagen ratios behave as expected for bones, which are known to have greatly differing mineral contents.[3] The present study, in which the mineral content was measured by biochemical means, also showed regional variation in composition which was in agreement with the Raman data. Figure 7(b) shows that a change in the Raman mineral-to-collagen ratio actually represents a change in the relative proportion, by weight, of mineral, protein, and water.

4.5 *Regional Phosphate-to-Carbonate Variations*

Figure 6 shows that there is a subtle difference between the composition of the bone apatite at the ends of the tibia and that in the shaft. As discussed above, there is evidence to suggest that increased carbonate inclusion in the apatite crystals reduce crystallinity and affect the mechanical properties of the bone.[19,47] Studies of aging in mice[21] and osteoporosis in humans[20] have shown increased phosphate-to-carbonate ratio to be accompanied by decreased mineral-to-collagen ratio and altered bone mechanical properties, specifically increased capacity to deform (mice), and fewer low-trauma fractures (osteoporosis in humans), i.e., tougher/less stiff bone. Whether the mechanical properties of bone material near the ends of long bones is tuned by composition or whether the carbonate inclusions are more likely to occur in the less mineralized bone cannot be addressed by the present study. That a broad flat Raman band associated with the organic phase of bone is known to overlap with the carbonate band (from ~1000 to ~1100 cm^{-1}) further complicates the analysis.

4.6 *Limitations and Future Directions*

As described above, variations along the length of long bones have been recorded using other analytical techniques (e.g., x-ray, ultrasound, gravimetric, collagen orientation, etc.). Comparisons of those techniques with the Raman data presented here provide scope for interesting future work.

Figures 3 and 4 show that the transition from more highly mineralized (i.e., stiffer) bone to the less mineralized bone (i.e., more pliant) is gradual, meaning there are no sharp interfaces between materials of very different Young's modulus and, thus, no large stress discontinuities. Future investigations will look at compositional trends in different long bones and look for differences related to gender or age. It would be interesting to know if a disruption in the trend (perhaps medically induced) would affect the bone's performance and lead to increased or decreased risk of fractures in the shaft.[48] If the variation in composition along the cephalocaudal axis was altered by disease and stiffer mid-shaft bone was formed near the end of the bone, it could lead to destructive forces being transmitted to the cartilage/joint each time the bone was loaded.[49,50] One could speculate that the loss of bone, or the adaptation to new loading conditions (e.g., muscle wastage), could alter the mineralization patterns in long bones. In this event, any regions that developed more highly mineralized materials would suffer from reduced toughness and greater susceptibility to microcracks and/or fracture. As spatially offset Raman spectroscopy is developed as a noninvasive tool for monitoring bone transcutaneously, it will be possible to explore these hypotheses *in vivo*.[25,36,51]

The results of the biochemical analysis in Fig. 7(b) hint that the compositional adaptation of bone material within a long bone fits the same paradigm as that of specialized functionally adapted bones from different creatures (i.e., bulla, antler, etc.).[1,2,7] If the composition of bone is an independent design parameter of bone matrix, then understanding how regions of bone (that are only separated by a few millimeters) can have such large variations in composition will be of interest. The cues (be they genetic or local) for osteoblast matrix synthesis may present novel therapeutic targets for controlling bone composition and, thus, bone's material properties.

5 Conclusions

For the first time, Raman spectroscopic mapping of whole bones has revealed a complexity of adaptation of form to function that was not fully appreciated previously. Raman mapping along long bones has shown, in fine spatial resolution, that the mineral-to-collagen ratio and the phosphate-to-carbonate ratio of mid-shaft bone is larger than that of distal/proximal bone. Biochemical analysis of tibiae has confirmed that the mid-shaft bone and more distal/proximal bone have different relative proportions, by weight, of the main constituents.

If the composition is an independent design parameter of bone matrix, then the controlling factors of osteoblast matrix synthesis (be they genetic or local cues) would be interesting to explore. The data in this paper will also be useful in developing Raman spectroscopy as a noninvasive tool for measuring bone composition *in vivo* and also to inform mathematical modeling of the mechanical adaptation seen in whole bones.

Acknowledgments

The authors would like to thank the Vesalius Clinical Training Centre at the Centre for Comparative and Clinical Anatomy at the University of Bristol for supplying the human bone samples. They would also like to thank the Engineering and Physical Sciences Research Council (EP/H002693/1), the Science and Technology Facilities Council's Biomed Network, and University College London for their support. The codes for the human tissue authority license and material transfer agreement for the tibiae were HTA12135 and 08/H072/34, respectively.

References

1. J. D. Currey, *Bones: Structure and Mechanics*, 2nd ed., Princeton University Press, Princeton, New Jersey (2006).
2. J. D. Currey, "Mechanical properties of bone tissues with greatly differing functions," *J. Biomech.* **12**(4), 313 (1979).

3. K. Buckley et al., "Raman spectroscopy reveals differences in collagen secondary structure which relate to the levels of mineralisation in bones that have evolved for different functions," *J. Raman Spectrosc.* **43**(9), 1237–1243 (2012).
4. S.S.J. Webster, "Integrated bone tissue physiology," Chapter 1 in *Bone Mechanics Handbook*, 2nd ed., S.C. Cowin, Ed., pp. 1–68, CRC Press, Boca Raton, Florida (2001).
5. A. A. Biewener, "Bone strength in small mammals and bipedal birds: do safety factors change with body size?," *J. Exp. Biol.* **98**, 289–301 (1982).
6. S. Lees, "Considerations regarding the structure of the mammalian mineralized osteoid from viewpoint of the generalized packing model," *Connect. Tissue Res.* **16**(4), 281–303 (1987).
7. P. Zioupos, J. D. Currey, and A. Casinos, "Exploring the effects of hypermineralisation in bone tissue by using an extreme biological example," *Connect. Tissue Res.* **41**(3), 229–248 (2000).
8. C. Les et al., "The distribution of material properties in the equine third metacarpal bone serves to enhance sagittal bending," *J. Biomech.* **30**(4), 355–361 (1997).
9. F.G. Evans and M. Lebow, "Regional differences in some of the physical properties of the human femur," *J. Appl. Physiol.* **3**(9), 563–572 (1951).
10. M. H. Pope and J. O. Outwater, "Mechanical properties of bone as a function of position and orientation," *J. Biomech.* **7**(1), 61–66 (1974).
11. R. B. Ashman et al., "A continuous wave technique for the measurement of the elastic properties of cortical bone," *J. Biomech.* **17**(5), 349–361 (1984).
12. H. D. Kim and W. R. Walsh, "Mechanical and ultrasonic characterization of cortical bone," *Biomimetics* **1**, 293–310 (1993).
13. R. H. Bonser, "Longitudinal variation in mechanical competence of bone along the avian humerus," *J. Exp. Biol.* **198**(Pt 1), 209–212 (1995).
14. P. J. Atkinson and J. A. Weatherell, "Variation in the density of the femoral diaphysis with age," *J. Bone Joint Surg. Br.* **49**(4), 781–788 (1967).
15. D. B. Burr, "Patterns of variability in mineralization of the primate femoral diaphysis," *Am. J. Phys. Anthropol.* **51**(2), 219–232 (1979).
16. E. Jansonsa et al., "Constructional peculiarities of the human tibia defined by reference to ultrasound measurement data," *Biomaterials* **5**(4), 221–226 (1984).
17. G. L. Mechanic et al., "Regional distribution of mineral and matrix in the femurs of rats flown on Cosmos 1887 biosatellite," *FASEB J.* **4**(1), 34–40 (1990).
18. F. S. L. Wong et al., "Mineral concentration gradients in rat femoral diaphyses measured by x-ray microtomography," *Calcif. Tissue Int.* **56**(1), 62–70 (1995).
19. M. D. Morris and G. S. Mandair, "Raman assessment of bone quality," *Clin. Orthop. Related Res.* **469**(8), 2160–2169 (2011).
20. B. R. McCreadie et al., "Bone tissue compositional differences in women with and without osteoporotic fracture," *Bone* **39**(6), 1190–1195 (2006).
21. O. Akkus, F. Adar, and M. B. Schaffler, "Age-related changes in physicochemical properties of mineral crystals are related to impaired mechanical function of cortical bone," *Bone* **34**(3), 443–453 (2004).
22. R. F. Capozza et al., "Structural analysis of the human tibia by tomographic (pQCT) serial scans," *J. Anat.* **216**(4), 470–481 (2010).
23. M. Kazanci et al., "Bone osteonal tissues by Raman spectral mapping: orientation—composition," *J. Struct. Biol.* **156**(3), 489–496 (2006).
24. M. Kazanci et al., "Raman imaging of two orthogonal planes within cortical bone," *Bone* **41**(3), 456–461 (2007).
25. M. D. Morris, "Raman spectroscopy of bone and cartilage," Chapter 14 in *Emerging Applications of Raman Spectroscopy in Pharmaceutical and Biomedical Fields*, P. Matousek and M. D. Morris, Eds., pp. 347–364, Springer, Berlin, Germany (2010).
26. C. A. Lieber and A. Mahadevan-Jansen, "Automated method for subtraction of fluorescence from biological Raman spectra," *Appl. Spectrosc.* **57**, 1363–1367 (2003).
27. H. L. Birch, A. J. Bailey, and A. E. Goodship, "Macroscopic 'degeneration' of equine superficial digital flexor tendon is accompanied by a change in extracellular matrix composition," *Equine Vet. J.* **30**(6), 534–539 (1998).
28. R. W. Farndale, D. J. Buttle, and A. J. Barrett, "Improved quantitation and discrimination of sulphated glycosaminoglycans by use of dimethylmethylene blue," *Biochim. Biophys. Acta* **883**(2), 173–177 (1986).
29. K. Buckley et al., "Millimetre-scale mapping of cortical bone reveals organ-scale heterogeneity," *Appl. Spectrosc.* **68**(4) (2014).
30. C. P. Tarnowski, M. A. Ignelzi, and M. D. Morris, "Mineralization of developing mouse calvaria as revealed by Raman microspectroscopy," *J. Bone Miner. Res.* **17**(6), 1118–1126 (2002).
31. K. A. Dooley et al., "Stress mapping of undamaged, strained, and failed regions of bone using Raman spectroscopy," *J. Biomed. Opt.* **14**(4), 044018 (2009).
32. J. A. Timlin, A. Carden, and M. D. Morris, "Chemical microstructure of cortical bone probed by Raman transects," *Appl. Spectrosc.* **53**(11), 1429–1435 (1999).
33. J. G. Ramasamy and O. Akkus, "Local variations in the micromechanical properties of mouse femur: the involvement of collagen fiber orientation and mineralization," *J. Biomech.* **40**(4), 910–918 (2007).
34. E. Donnelly et al., "Effects of tissue age on bone tissue material composition and nanomechanical properties in the rat cortex," *J. Biomed. Mater. Res. A* **92**(3), 1048–1059 (2010).
35. S. Gamsjaeger et al., "Cortical bone composition and orientation as a function of animal and tissue age in mice by Raman spectroscopy," *Bone* **47**, 392–399 (2010).
36. M. V. Schulmerich et al., "Noninvasive Raman tomographic imaging of canine bone tissue," *J. Biomed. Opt.* **13**(2), 020506 (2008).
37. D. B. Kimmel and W. S. Jee, "A quantitative histologic study of bone turnover in young adult beagles," *Anat. Rec.* **203**, 31–45 (1982).
38. G. Marotti, "Quantitative data on bone formation rate throughout the skeletal system," in *CISM Bone Cell and Tissue Mechanics*, Udine, Italy, pp. 19–23 (2010).
39. R. Amprino and G. Marotti, "A topographic quantitative study of bone formation and reconstruction," in *Bone and Tooth*, J. J. Blackwood, Ed., pp. 21–23, MacMillan Co., New York (1964).
40. Z. F. G. Jaworski, "Does the mechanical usage (MU) inhibit bone 'remodeling'?," *Calcif. Tissue Int.* **41**, 239–248 (1987).
41. S. Carando et al., "Orientation of collagen in human tibial and fibular shaft and possible correlation with mechanical properties," *Bone* **10**(2), 139–142 (1989).
42. J. K. Gong, J. S. Arnold, and S. H. Cohn, "Composition of trabecular and cortical bone," *Anat. Rec.* **149**(3), 325–331 (1964).
43. R. Hodgskinson, J. D. Currey, and G. P. Evans, "Hardness, an indicator of the mechanical competence of cancellous bone," *J. Orthop. Res.* **7**(5), 754–758 (1989).
44. S. R. Goodyear et al., "A comparison of cortical and trabecular bone from C57 Black 6 mice using Raman spectroscopy," *Bone* **44**(5), 899–907 (2009).
45. X. E. Guo and S. A. Goldstein, "Is trabecular bone tissue different from cortical bone tissue?," *Forma* **12**, 185–196 (1997).
46. D. Pienkowski et al., "Calcitonin alters bone quality in beagle dogs," *J. Bone Miner. Res.* **12**(11), 1936–1943 (1997).
47. J. S. Yerramshetty and O. Akkus, "The associations between mineral crystallinity and the mechanical properties of human cortical bone," *Bone* **42**(3), 476–482 (2008).
48. J. Schilcher, K. Michaëlsson, and P. Aspenberg, "Bisphosphonate use and atypical fractures of the femoral shaft," *N. Engl. J. Med.* **364**(18), 1728–1737 (2011).
49. D. B. Burr, The importance of subchondral bone in the progression of osteoarthritis," *J. Rheumatol. Suppl.* **70**, 77–80 (2004).
50. T. Buchwald et al., "Identifying compositional and structural changes in spongy and subchondral bone from the hip joints of patients with osteoarthritis using Raman spectroscopy," *J. Biomed. Opt.* **17**(1), 017007 (2012).
51. K. Buckley et al., "Decomposition of in vivo spatially offset Raman spectroscopy data using multivariate analysis techniques," *J. Raman Spectrosc.* (2014).

Kevin Buckley is a laser spectroscopy scientist at the Science & Technology Facilities Council's Central Laser Facility at Harwell, Oxfordshire. In 2011, he was awarded a PhD by University College London (UCL) for his work on the Raman spectroscopy of bone. Previously, he graduated from University College Cork/Tyndall National Institute, Ireland, with an MSc degree (novel semiconductor laser devices), a postgraduate diploma (applied physics), and a BSc degree (chemical, mathematical, and physical sciences).

Jemma G. Kerns received her BSc (Hons) in natural sciences and PhD in biological sciences at Lancaster University in 2007 and 2010, respectively. She has been a research associate at UCL since October 2010. Currently, she is developing spatially offset Raman spectroscopy for use *in vivo*, including developing protocols and robust computational methodologies for spectral processing and analysis. She is particularly interested in the translation of these techniques into a clinical setting for high-throughput diagnosis of medical conditions.

Helen L. Birch is a senior lecturer in musculoskeletal pathobiology at UCL. Having graduated with a BSc (Hons) in biochemistry and physiology from Cardiff University, she continued studies at Bristol University on tendon biology, gaining a PhD in 1993. Her expertise is in extracellular matrix biochemistry and her research activity is focused on understanding the relationship between structure and function in skeletal tissues, particularly tendon, and also in other tissues, such as ligament and bone.

Panagiotis D. Gikas graduated from St. George's Hospital Medical School in 2003 and was awarded his MD from UCL in 2013. He is currently specializing in orthopedic oncology. He has a keen interest in the use of Raman spectroscopy for the diagnosis of musculoskeletal disease and is aiming to develop this technique for use in various fields of orthopedics, predominantly oncology and degenerative disease.

Anthony W. Parker is a physical chemist with expertise in the characterization of complex chemical and biological systems using temporal and spatial, spectroscopic and imaging, laser-based methods. As coinventor of spatially offset Raman spectroscopy, he keenly developed its application for diagnosis of disease. He is an STFC research fellow with academic positions at UCL, University of Stellenbosch, University of Salford, and associate editor of *Journal of Raman Spectroscopy*.

Pavel Matousek has worked at the Rutherford Appleton Laboratory since 1991. He pioneered the concepts of Kerr gated Raman fluorescence rejection and spatially offset Raman spectroscopy. His honors include 2009 Charles Mann Award and 2002 and 2006 Meggers Awards. He is a fellow of the Royal Society of Chemistry, a senior fellow of STFC, a visiting professor at the UCL, and a founding director of Cobalt Light Systems.

Allen E. Goodship graduated in veterinary science and, after a PhD in functional adaptation of bone, has pursued a research interest in the pathobiology of skeletal tissues and comparative musculoskeletal science. He has been president of the British Orthopaedic Research Society and the International Society for Fracture Repair. He was director of the UCL Institute of Orthopaedics and Musculoskeletal Science and now holds professorial appointments at both UCL and the University of Bristol.